ELSEVIER

Nuclear Instruments and Methods in Physics Research B 147 (1999) 244–248

NIM B
Beam Interactions
with Materials & Atoms

Stability studies of Hg implanted $YBa_2Cu_3O_{6+x}$

J.P. Araújo [a,b,*], J.G. Correia [b,c], U. Wahl [d], J.G. Marques [c,e], E. Alves [e], V.S. Amaral [a], A.A. Lourenço [f], V. Galindo [g], T. von Papen [g], J.P. Senateur [g], F. Weiss [g], A. Vantomme [d], G. Langouche [d], A.A. Melo [c], M.F. da Silva [e], J.C. Soares [c], J.B. Sousa [a], ISOLDE Collaboration [b]

[a] *IFIMUP, Dep. Física, Faculdade de Ciências, Rua do Campo Alegre 687, P-4150 Porto, Portugal*
[b] *CERN, CH-1211 Geneva 23, Switzerland*
[c] *CFNUL, Av. Prof. Gama Pinto 2, P-1699 Lisboa Codex, Portugal*
[d] *Instituut voor Kern- en Stralingsfysica, Celestijnenlaan 200 D, B-3001 Leuven, Belgium*
[e] *Instituto Tecnológico e Nuclear, Estrada Nacional 10, P-2685 Sacavém, Portugal*
[f] *INESC, Rua Campo Alegre 687, P-4150 Porto, and Dep. Física, University Aveiro, P-3800 Aveiro, Portugal*
[g] *UMR CNRS 5628, INPG-ENSPG, BP 46-38402 St. Martin D'Hères, Cedex, France*

Abstract

High quality $YBa_2Cu_3O_{6+x}$ (YBCO) superconducting thin films were implanted with the radioactive ^{197m}Hg ($T_{1/2} = 24$ h) isotope to low fluences of 10^{13} atoms/cm^2 and 60 keV energy. The lattice location and stability of the implanted Hg were studied combining the Perturbed Angular Correlation (PAC) and Emission Channeling (EC) techniques. We show that Hg can be introduced into the YBCO lattice by ion implantation into a unique regular site. The EC data show that Hg is located on a highly symmetric site on the YBCO lattice, while the PAC data suggests that Hg occupies the Cu(1) site. Annealing studies were performed under vacuum and O_2 atmosphere and show that Hg starts to diffuse only above 653 K. © 1999 Elsevier Science B.V. All rights reserved.

PACS: 68.55.L; 74.62.D; 74.76
Keywords: Ion implantation; Thin films; High-T_c superconductors; Doping; Nuclear techniques

---

1. Introduction

The $YBa_2Cu_3O_{6+x}$ (YBCO) compound is one of the most studied and interesting high-T_C superconductor materials. Doping studies have shown that the superconducting properties of YBCO are always degraded, except when doping with Au or Hg, which increase T_C by 2 K [1] and 10 K [2]. In these studies Hg was introduced to several percent during sintering by changing the composition of the reactants. Therefore the Hg site was not known, and the presence of different crystalline phases cannot be excluded.

In the present work radioactive ^{197m}Hg was introduced into YBCO thin films by ion implantation to very low fluences. The atomic environment

---

[*] Corresponding author. Tel.: 41 22 767 6491/9709; fax: 41 22 767 8990; e-mail: joao.pedro.esteves.de.araujo@cern.ch

PII: S0168-583X(98)00544-8

of Hg and its lattice site position were studied with the $e^{-}-\gamma$ Perturbed Angular Correlation (PAC), and Emission Channeling (EC) nuclear techniques [3]. For control, the critical temperature (T_c) was measured with the Alternate Susceptibility (χ_{ac}) technique in the as-grown state and after the implantation and annealing treatments.

2. Experimental details

Poly- and [0 0 1] single-crystalline high quality YBCO thin films (100–350 nm) were deposited by Pulsed Laser Ablation or MOCVD on [1 0 0] $SrTiO_3$ substrates. The crystalline quality was checked by Rutherford Backscattering/Channeling and X-ray diffraction. The ^{197m}Hg radioactive isotope was implanted into the films at room temperature (RT) and 60 keV energy at the ISOLDE facility [4]. To avoid the production of unknown crystalline phases the beam was swept to get homogeneously low fluences of 1.0×10^{13} Hg/cm^2. The Hg projected range is $R_P = 16$ nm, and its peak concentration 7×10^{18} at/cm^3 [5], i.e. about 0.01 at.%. The implanted samples were firstly annealed in vacuum (3×10^{-6} mbar), increasing the temperature from RT up to 757 K in 100 K steps of 10 h each. PAC measurements were made after implantation and during vacuum annealing. Subsequently the samples were annealed at 723 K under O_2 flow (1 bar). The temperature was increased from RT to 723 K in 30 min and after 6 h annealing, slowly decreased (1 K/min) back to RT.

The PAC measurements were performed using the well-known 165–134 keV cascade from the decay of the 24 h half-life ^{197m}Hg isomeric state [6]. Details of the experimental setup and procedures can be found in Ref. [7]. The PAC technique is particularly suitable to probe the vicinity of the implanted Hg nuclei at an atomic level [8]. Its sensitivity is given by the electric field gradient (EFG) which is caused by the deviation from cubic symmetry of the charge distribution around the probes. This results in a modulation of the PAC spectrum, $R(t)$. For a cascade with an intermediate level with spin $I = 5/2$, three frequencies are observable per EFG. From these frequencies the coupling constant of the interaction, $\nu_Q = eQV_{zz}/h$, and the asymmetry parameter $\eta = (V_{xx} - V_{yy})/V_{zz}$ are extracted. V_{zz} is the principal component of the EFG tensor, which is produced from the extra nuclear charge distribution. $Q = -0.057 \pm 0.007$ b is the quadrupole moment of the 134 keV excited state. The interaction with randomly distributed defects does not lead to the measurement of a sharp frequency, but rather to a distribution of frequencies. Here we assume such distributions to be Lorentzian-like, with average value $\langle \nu_Q \rangle$ and standard deviation σ_Q, depending on the density and variety of the lattice defects.

The EC experiments were performed after implantation by measuring the yield of the L + M conversion electrons from both the 165 and 134 keV transitions, as a function of angle towards the [0 0 1] crystallographic direction. For this purpose we used 30×30 mm^2 position sensitive detectors developed at CERN for high-energy physics experiments and recently adapted for the present use [9].

3. Results

Fig. 1 shows $R(t)$ spectra measured at several temperature steps up to 757 K. All spectra were fitted assuming one frequency distribution centered at $\langle \nu_{Q1} \rangle = 122 \pm 1$ MHz. In Fig. 2 σ_Q and η are plotted as a function of annealing/measuring temperature. σ_Q decreases strongly from $\sigma_Q = 29 \pm 2$ MHz (as-implanted) to 6.6 ± 0.6 MHz ($T_M = 511$ K), enhancing the amplitude of the $R(t)$ spectra (Fig.1). The strong attenuation of the as-implanted spectrum is due to Hg nuclei that interact with randomly distributed defects. Within our range of sensitivity, a few nanometers around the Hg probe nuclei, we identify one annealing step at 511 K where the lattice recovers and no point defects are in the neighborhood of the probes. The η parameter vanishes for annealing temperatures above 511 K.

The Hg stability was studied measuring the γ count rate of the 134 keV transition and the PAC coincidence rate. No losses were observed up to 653 K. Above this temperature Hg starts to diffuse. During annealing at 757 K both the γ and the PAC coincidence rates had the same relative decrease,

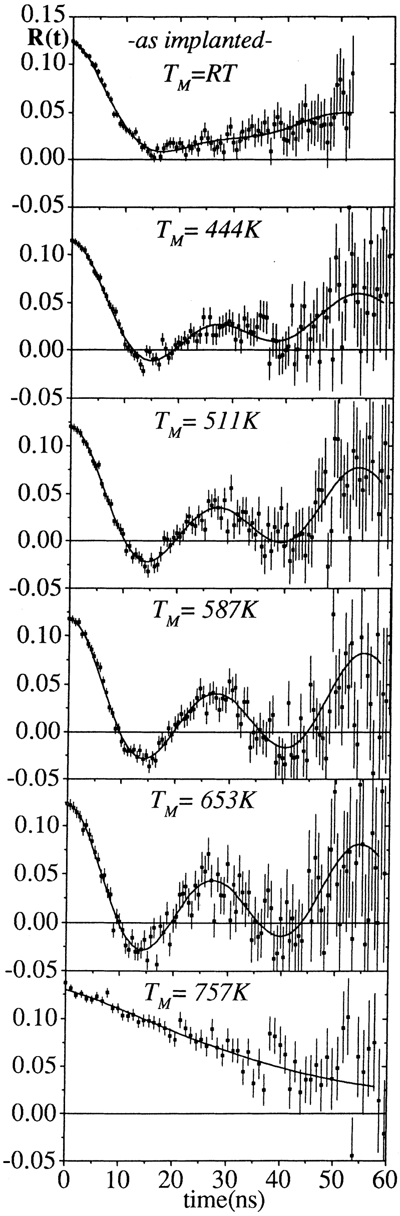

Fig. 1. PAC spectra measured after implantation and during annealing in vacuum up to 757 K.

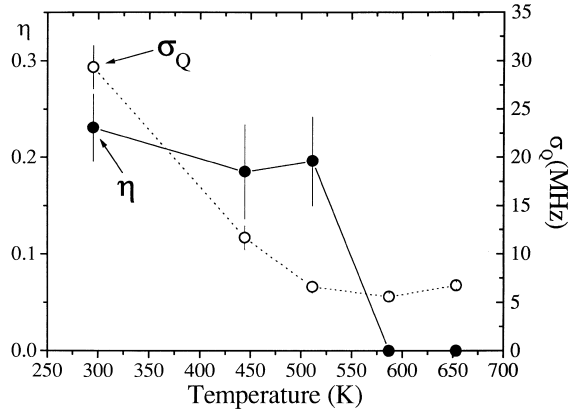

Fig. 2. Plot of the standard deviation σ_Q, and the asymmetry parameter η as a function of annealing/measuring temperature in vacuum.

indicating a strong out-diffusion of Hg. If Hg would only diffuse within the film, the coincidence rate would decrease at a higher rate than the γ rate, due to a higher absorption and scattering of the conversion electrons through the film. At 757 K the diffusion was still slow and the Hg losses small enough to measure an 8 h long $R(t)$ spectrum (Fig.1), which displays a different pattern, characterized by $\langle \nu_{Q2} \rangle = 23 \pm 3$ MHz and $\sigma_{Q2} = 25 \pm 9$ MHz. This change was shown to be irreversible when returning to measurements at temperatures lower than 653 K. We further checked that all the remaining activity was still on the film. Thus the $R(t)$ spectrum taken at 757 K is due to Hg atoms which are no more in the initial lattice sites but are still in the YBCO lattice.

Fig. 3 shows the normalized conversion electron yields measured after implantation, as a

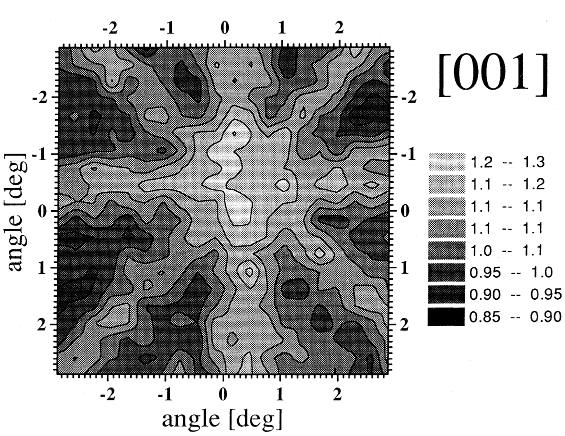

Fig. 3. Normalised conversion electron intensities measured off the [0 0 1] direction, after implantation.

function of the angle off the [001] axis. The increase of the electron yield along the [001] axis reveals that Hg lies along the *c*-axis either on the Y/Ba or the Cu rows, since EC effects along pure O rows are expected to be much less pronounced. This agrees with the high symmetry of the ^{197}Hg (YBCO) EFG, whose principal component (V_{zz}) was found to be aligned with the [001] axis [10]. New EC experiments investigating different crystalline axes are in progress.

Fig. 4 shows the in-phase component of the alternate susceptibility (χ') measured as a function of temperature in the as-grown film, after implantation and subsequent annealing in vacuum up to 757 K, and after subsequent annealing at 723 K for 6 h under flowing O_2. As expected, the sample didn't show the superconducting phase transition after annealing in vacuum. The oxygen losses should have caused the orthorhombic–tetragonal structural phase transition, thus transforming the superconductor compound into an antiferromagnetic insulator. Superconductivity was recovered after 6 h annealing at 723 K under O_2 flow. The structure that is seen in the χ' curve after annealing in oxygen, is most likely due to inhomogeneous O doping.

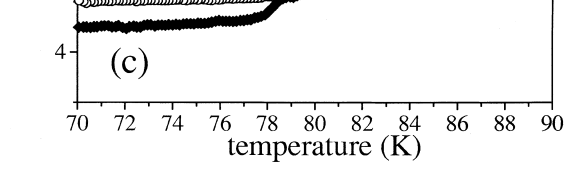

Fig. 4. In-phase component of alternate susceptibility (χ_{ac}) measured: (a) as deposited; (b) after Hg implantation and subsequent annealing in vacuum (no superconductor transition was found down to 20 K), and (c) after subsequent annealing under flowing O_2.

4. Discussion and conclusions

The results presented here were shown to be fully reproducible for all thin films we studied, independent of their production method. After implantation the Hg probes are already in unique lattice sites but are still interacting with randomly distributed defects. When annealing up to 653 K, 100% of the implanted Hg atoms remain on the same site, with no more point defects in its neighborhood. In the same temperature range the fundamental frequency ν_{Q1} didn't show any relevant change. This behavior can be understood by the fact that the lattice parameters should not show appreciable changes, although the orthorhombic–tetragonal phase transition can occur due to the annealing in vacuum [11]. Then η should be more sensitive to the phase transition. We have shown that when annealing under O_2 flow at 723 K [10], or by annealing in vacuum at temperatures below 511 K [this work], Hg occupies a regular lattice site with charge symmetry lower than tetragonal ($\eta = 0.20$). When annealing in vacuum at temperatures above 511 K η vanishes to zero, revealing that the Hg site symmetry changed to tetragonal. In previous work where the oxygen diffusion coefficient (D_O) was studied for thin films in O_2 atmosphere [12], it was found that oxygen starts to migrate, being exchanged with the atmosphere, above 523 K. By using $D_O(588\text{ K}) \sim 1.5\times10^{-13}$ cm^2/s we estimated the diffusion length for a 10 h long annealing, $L = (D_O\ t)^{1/2} = 735$ nm, which is much larger than the film thickness. The χ_{ac} measurements performed after annealing in vacuum have shown that the films were no more superconducting. Then the superconducting transition was reestablished after annealing in O_2 flow, reinforcing the interpretation that oxygen was released during annealing in vacuum to a relative content $x<0.4$ on the $YBa_2Cu_3O_{6+x}$ structure. Thus we interpret the vanishing of η as being due to the orthorhombic–tetragonal YBCO structural phase transition, which occurred in our thin films between 511 and 587 K.

The EC results show that Hg lies along the Cu or Y/Ba *c*-axis rows. It is known that Hg has a big affinity to form linear-like coordinated bonds, e.g., in the $Hg_1Ba_2Ca_{(n-1)}Cu_nO_{(2n+2+\delta)}$ high-*T*c superconductor family and in HgO. In both cases

Hg has two linearly coordinated (apical) oxygen atoms as its first neighbors. Moreover, the ratio $|\nu_Q/Q| = |eV_{zz}/h| = 2140 \pm 263$ MHz b^{-1} found in this work is very close to the value $|eV_{zz}/h| = 1829 \pm 210$ MHz b^{-1}, found for ^{199}Hg : HgO [13]. Then the lattice contribution for the EFG is in first order proportional to the ratio $R_{\mathrm{Hg}} = V_{zz}/(1-\gamma_\infty) = 14.6$ V/Å^2, where $(1-\gamma_\infty)$ is the Sternheimer antishielding coefficient that accounts for the EFG enhancement due to the polarization of the probe's (Hg) electronic core [14,15]. Taking equivalent ratios from the EFGs calculated for different lattice sites in YBCO$_{6(x=0)}$ [16], we find $R_{\mathrm{Cu(1)}} = 13.5$ V/Å^2, $R_{\mathrm{Cu(2)}} = 4.2$ V/Å^2, $R_{\mathrm{Ba}} = 1.4$ V/Å^2, and $R_{\mathrm{Y}} = 1.1$ V/Å^2. Thus the Cu(1) YBCO lattice site appears as the most favorable to be occupied by the Hg ions.

When annealing above 653 K Hg starts to diffuse out slowly and the $R(t)$ spectra changes irreversibly. The Hg diffusion mechanism is not known. However, the very low value of $\langle\nu_{Q2}\rangle \sim 23 \pm 3$ MHz suggests that Hg is no more bound to oxygen and occupies low EFG lattice sites in the YBCO lattice. Finally, the abundance of oxygen seems to delay this diffusion, since in a previous work we have shown that after annealing under O_2 flow a small amount of Hg was lost at 723 K and ν_Q did not change [10].

In conclusion, in this work we have applied the PAC and EC nuclear techniques to study the stability and lattice site of implanted Hg into YBCO thin films. We found that Hg occupies one unique lattice site, which is stable up to 653 K. Both the EC and the PAC results suggest that Hg occupies a highly symmetric lattice site, most likely the Cu(1) site, bonded to two apical oxygen atoms. A first annealing step of the implantation defects was found at 511 K. The orthorhombic–tetragonal phase transition occurred between 511 and 587 K under vacuum annealing. Hg diffusion starts only above 653 K. The PAC results at 757 K show that Hg is no more bound to oxygen and is now occupying higher symmetry sites in the YBCO lattice.

Acknowledgements

This work was partially funded by FCT, Portugal, through projects CERN/S/FIS/1048/95, PBICT/C/CTM/1891/9 and grants under the PRAXIS XXI Programme (J.P.A., J.G.C. and J.G.M.).

References

[1] G. Ganakas, M.J. Morgan, G. Jakovidis, J. Mater. Sci.: Mater. Electr. 6 (1995) 244.
[2] A.K. Chakraborty, K. Bose, G. Som, B.K. Chaudhuri, J. Mater. Sci.: Mater. Electr. 5 (1994) 22.
[3] J.G. Correia, Nucl. Instr. and Meth. B 136–138 (1998) 736.
[4] E. Kugler, D. Fiander, B. Jonson, H. Haas, A. Przewloka, H.L. Ravn, D.J. Simon, K. Zimmer, ISOLDE Collaboration, Nucl. Instr. and Meth. B 70 (1992) 41.
[5] J.F. Ziegler, J.P. Biersack, U. Littmark, in: The Stopping and Range of Ions in Solids, Pergamon, New York, 1985.
[6] W. Tröger, T. Butz, P. Blaha, K. Schwarz, Hyp. Int. 80 (1993) 1109.
[7] J.G. Marques, J.G. Correia, A.A. Melo, M.F. da Silva, J.C. Soares, ISOLDE Collaboration, Nucl. Instr. and Meth. B 99 (1995) 645.
[8] Th. Wichert, N. Achziger, H. Metzner, R. Sielemann, Perturbed angular correlation, in: G. Langouche (Ed.), Hyperfine Interactions of Defects in Semiconductors, Elsevier, Amsterdam, 1992, p. 1.
[9] U. Wahl, J.G. Correia, S. Cardoso, J.G. Marques, A. Vantomme, G. Langouche, ISOLDE Collaboration, Nucl. Instr. and Meth. B 136–138 (1998) 744.
[10] V.S. Amaral et al., J. Magn. Mag. Mater. 177–181 (1998) 511.
[11] J.D. Jorgensen et al., Phys. Rev. B 36 (1987) 3608.
[12] Y. Li, J.A. Kilner, T.J. Tate, M.J. Lee, R.J. Chater, H. Fox, R.A. De Souza, P.G. Quincey, Phys. Rev. B 51 (1995) 8498.
[13] T. Butz, Th. Völkel, O. Nuyken, Chem. Phys. 149 (1991) 437.
[14] R.S. Raghavan, E.N. Kaufmann, P. Raghavan, Phys. Rev. Lett. 34 (1975) 1280.
[15] R.P. Gupta, S.K. Sen, Phys. Rev. A 8 (1973) 1169; F.D. Feiock, W.R. Johnson, Phys. Rev. 187 (1969) 39.
[16] K. Schwarz, C. Ambrosch-Draxl, P. Blaha, Phys. Rev. B 42 (1990) 2051.